2022 26th International Conference on Pattern Recognition (ICPR)
August 21-25, 2022, Montréal, Québec, Canada

WiID: Precise WiFi-based Person Identification via Bio-electromagnetic Information

Mingda Han, Linlin Guo*, Jia Zhang*, Hui Ji, Zihan Diao and Jiande Sun
School of Information Science and Engineering
Shandong Normal University, Jinan, China
Email: mingdahan@outlook.com, linlin.teresa.guo@gmail.com, zhangjia@sdnu.edu.cn,
hui.ji@sdnu.edu.cn, hyxxdzh123@163.com, jiandesun@hotmail.com

2022 26th International Conference on Pattern Recognition (ICPR) | 978-1-6654-9062-7/22/$31.00 ©2022 IEEE | DOI: 10.1109/ICPR56361.2022.9956619

Abstract—**From the perspective of privacy protection and convenience, WiFi-based person identification in wireless sensing has attracted extensive attention in recent years. In this paper, we propose a WiFi-based person IDentification (WiID) method, which can capture people's valid physiological information from Channel State Information (CSI) of different spatial streams even when people are in motion. The key idea is to detect and extract the short-time static states from the collected CSI and achieve person identification based on these short-time signals. By designing a Motion Sensitivity Vector (MSV) conversion algorithm, WiID is able to segment CSI that carries individual physiological information automatically without the individual performing an assigned action or maintaining a specific state. As far as we know, it is the first work that enables precise person identification using people's physiological information when people do not keep stationary. Experimental results in real-life scenarios show that WiID can achieve 92.65% of average accuracy in three different environments.**

I. Introduction

Growing attention has been drawn to the domain of WiFi sensing especially on activity detection and recognition [1–7], indoor positioning and tracking [8–11], and person identification [12–19]. Person identification based on WiFi measurements in these areas has been widely applied to indoor smart sensing environments. Compared to the traditional identification applications depending on personal biometric features, such as the face and iris, person identification using wireless signals can break through the limitations of the Line-of-Sight (LoS) environment and alleviate the growing privacy concerns.

With the extensive deployment of low-cost off-the-shelf WiFi devices in current indoor environments, numberous researchers focus on using existing WiFi devices for person identification. In the literature, person identification methods using WiFi signals are divided into two categories, which are behavior-based and bio-electromagnetic-based. Behavior-based person identification method leverages the one-to-one correspondence between the WiFi signal patterns and the human behavior patterns for identification. Bio-electromagnetic-based person identification method exploits the influence of personal physiological characteristics on WiFi signals transmission. When the WiFi signals pass through the layers of tissue in the human body, the human body of each layer of tissue will have a different influence on the attenuation and travel time of the received signals. Due to individual differences, such as different human body shapes, total body water volume, skin conditions, different people will also have different influences on the received WiFi signals.

Behavior patterns (e.g., gait, daily activities, etc.) of people can be imitated and are prone to change in certain specific circumstances (e.g., injury, weight bearing, etc.), while the physiological characteristics remain relatively stable, as it can reflect the property of the human body. Therefore, bio-electromagnetic-based methods are more reliable. However, the weak physiological information is easily overwhelmed by action during data acquisition. Hence, most of the existing bio-electromagnetic-based methods require the users to remain as stationary as possible during data acquisition.

In order to accurately capture the weak physiological information from the received WiFi signals, we design a series of signal denoising and transformation algorithms to extract short-time static states from the motion state of the person. Approximately, we assume that the Channel State Information (CSI) collected at stationary state contains only physiological information of the individual. Therefore, we first need to precisely distinguish the different effects of people's physiological information and their movement information and then determine the boundary of signal patterns reflected off the stationary human from the collected data. In order to better describe signal change patterns caused by the human body, we harness Multiple-Input Multiple-Output (MIMO) technique to capture the CSI from nine spatial streams and then extract efficiently signal change representation for distinguishing a person's two states (e.g., stationary state and motion state). Based on the analysis above, we propose WiID to quickly detect and identify the moving people using commercial WiFi devices.

The main contributions of this paper are as follows:

- We propose WiID, a bio-electromagnetic-based WiFi person identification method that achieves identification even when the person is in motion. We creatively decompose an identification process into multiple sub-states to extract valid physiological information.
- We design a signal conversion algorithm to obtain the Motion Sensitivity Vector (MSV), which helps segment the raw data automatically to get valid bio-electromagnetic information.

*Corresponding author.

- We evaluate WiID using extensive experiments of different factors. The experimental results show that our method can achieve an average accuracy of 100% to 95.25% from a group of 2 to 14 people, respectively.

The rest of the paper is organized as follows. We first review the related work in Section II and introduce the system framework in Section III. Then, the experiments and evaluation are given in Section IV. Finally, we conclude the paper in Section V.

II. Related Work

WiFi-based human sensing focuses on exploring the effect of human on WiFi signals. Hence, the relevant prior work includes WiFi-based activity detection and recognition and WiFi-based person identification.

A. WiFi-based Activity Detection and Recognition

WiFi-based activity detection and recognition can be divided into two categories, which are coarse-grained and fine-grained. Coarse-grained activity detection and recognition is mainly for activities with a relatively large range of movements, such as fall, walking, standing, sitting, etc. While fine-grained activity detection and recognition is mainly for activities with small action magnitude, such as gestures, keystrokes, etc. Vital signs (e.g., respiration, heartbeat, etc.) monitoring is essentially a fine-grained activity detection task as well.

Early researchers use coarse-grained Received Signal Strength Index (RSSI) for activity detection and recognition [5]. With the modification of the Intel 5300 NIC by Halperin et al. [20], a large number of researchers have started to use fine-grained CSI for activity detection and recognition. RT-fall [6] is the first work to use the phase difference of CSI from different antennas for fall and fall-like activities detection, and to implement fall detection by machine learning algorithms. E-eyes [7] leverages the amplitude distribution of CSI as a feature and combines Empirical Mode Decomposition (EMD) and Dynamic Time Warping (DTW) algorithms to achieve activity recognition. Meanwhile, with the development of deep learning techniques, researchers start to combine deep learning techniques to improve the fineness of activity recognition. Daqing Zhang's team proposes the Fresnel Zone model [4] for the first time in the field of WiFi sensing, which provides a theoretical basis for WiFi sensing tasks and effectively improves the accuracy and stability of sensing by combining deep learning techniques.

B. WiFi-based Person Identification

Behavior-based person identification. Behavior-based identification is mainly dependent on the behavior patterns (e.g., gait, etc.) which are different from person to person. It is essentially a more fine-grained activity recognition task.

Jie Wang *et al.* propose an EMD based general Device-Free Identification (DFI) framework and design a DFI system based on gait and respiration characteristics under the guidance of this framework [14]. WiWho [12] and WiFi-ID [13] are the first to extract time domain or frequency domain features of user's gait in WiFi CSI for person identification. However, early works have great dependence on the walking path. To break the walking path limitation, WiDIGR [21] and WiPIGR [17] utilize multiple transceiver pairs and propose a series of signal processing techniques to eliminate path-dependent features, and finally obtain path-independent spectral features through spectrogram optimization and combine Convolutional Neural Network (CNN) and Long Short-Term Memory (LSTM) network for path independent gait recognition. Belal Korany *et al.* propose a multi-dimensional framework spanning time, frequency and space domains, which can extract the corresponding gait information of each walker, thus realizing the identification of multiple individuals through walls [16].

Bio-electromagnetic-based person identification. Unlike the above behavior-based method, bio-electromagnetic-based method does not require the identified person to do any specific actions or behavior. This kind of identification system is based on fundamental principles in bio-electromagnetic which focuses on the influence of biological tissues on electromagnetic (EM) waves.

Qinyi Xu *et al.* use Time-Reversal (TR) technology to extract useful human bio-electromagnetic information from the processed WiFi signals and leverage the strength of the spatial-temporal resonances for through-wall human identification [18]. In [19], Fei Wang *et al.* preprocess the raw signal to mitigate the multipath effect and leverage 30 subcarriers and their time-domain statistical characteristics to identify legal users while rejecting illegal users through Support Vector Machine (SVM) and threshold learning. However, state-of-the-art bio-electromagnetic-based person identification methods require the user to remain strictly stationary and fail to work in situations where the user is moving.

III. System Design

A. System Overview

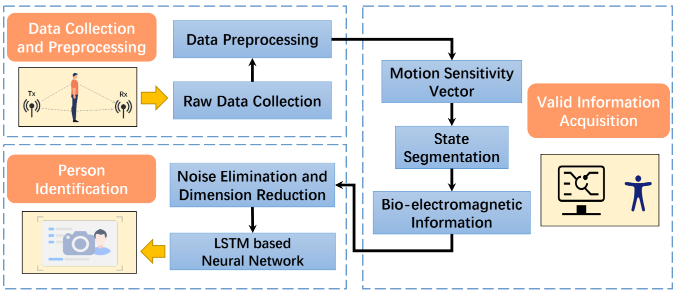

Fig. 1: System overview

In order to achieve accurate person identification with commercial WiFi devices, we design a light-weighted person identification system. As shown in Fig. 1, the system contains three main modules, which are the data collection and preprocessing module, the valid information acquisition module, and the person identification module. The data collection and preprocessing module is responsible for raw CSI data collection and data preprocessing (e,g., denoising and outlier removal). Then, in the valid information acquisition module, the bio-electromagnetic information is extracted through Motion

Sensitivity Vector (MSV) conversion, state segmentation, and bio-electromagnetic information combination. Finally, person identification is carried out in the last module, where the de-noised data is fed into an LSTM neural network to extract the hidden features and complete the multi-category task.

B. Data Collection and Preprocessing

We obtain the CSI of nine spatial streams from a 3×3 MIMO transceiver, each of which has 30 Orthogonal Frequency Division Multiplexing (OFDM) subcarriers. Hence, we have a total of $3 \times 3 \times 30 = 270$ CSI values for each received 802.11n frame. The raw CSI of 30 subcarriers from one spatial stream is shown in Fig. 2(a).

The representation of CSI in time domain is the channel response $H(t)$, which we received at time t can be expressed as

$$H(t) = H_h(t) + H_e(t), \tag{1}$$

where $H_h(t)$, defined as the human component, carries the human bio-electromagnetic information, and $H_e(t)$ is generated from the environment. In this paper, we choose $H_h(t)$ for person identification, since it has the major influence on the received CSI when the transmission environment is unchanged.

As specified in [22], $H_h(t)$ can be expressed as

$$H_h(t) = \sum_{n \in \mathbb{P}} \alpha_n e^{-j\phi_n} \delta(t - \tau_n), \tag{2}$$

where α_n, ϕ_n and τ_n refer to the overall attenuation, the phase offset, and the delay at time t between the transceiver on the n-th path respectively. $\mathbb{P}$ denotes the set of all multipaths that go through the human body. We choose α_n as the valid information because we only use the amplitude information in the identification process. α_n is a complicated parameter, which depends on the antenna gain, propagation distance and attenuation characteristics of the obstacles [22]. The antenna gain and the propagation distance are predetermined once we fix the transceiver in each experimental environment. The attenuation characteristics of the human body depend on permeability, relative permittivity, and conductivity, which differ from person to person due to the different physiological characteristics [23–25]. Hence, we use these physiological information reflected in the CSI for person identification.

Due to the hardware imperfection and the multipath transmission, the collected raw CSI contains a large number of noise and outliers. We leverage the Hampel identifier and the Butterworth low pass filter to remove the outliers and high frequency noise. The preprocessed data is shown in Fig. 2(b). Compared to the raw data in Fig. 2(a), preprocessed data eliminates lots of outliers and the trend of the data is more obvious.

C. Valid Information Acquisition

We propose a novel algorithm that can segment the raw CSI data with the designed MSV to extract bio-electromagnetic information from the short-time static states automatically even when the person is in the motion state.

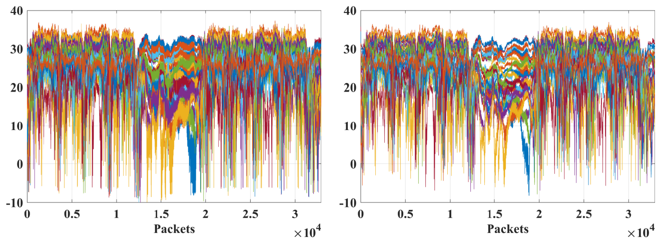

(a) Raw data (b) Preprocessed data

Fig. 2: Data collection and preprocessing

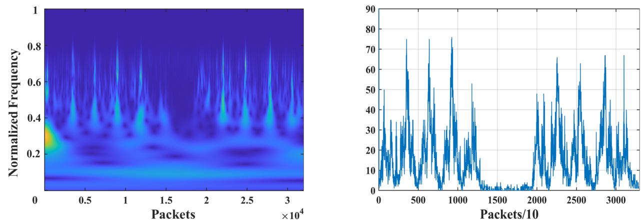

(a) Spectrogram (b) MSV

Fig. 3: Spectrogram v.s. Motion sensitivity vector

1) Motion Sensitivity Vector: As illustrated in Fig. 3(a), the conventional spectrogram method doesn't perform state segmentation well because there is no significant frequency difference between the static state and motion state. Meanwhile, the spectrogram method requires a fast packet rate. We propose to magnify the difference between the motion and static state by defining an MSV.

We obtain the variance matrix $\boldsymbol{V}_{3\times30\times L}$ by a variance-based sliding window method with a window size of 10 as follows

$$\boldsymbol{V}_{3\times30\times L} = getVarMatrix(\boldsymbol{C}^1_{3\times30\times N}), \tag{3}$$

where $L = \lfloor N/10 \rfloor$ and $\boldsymbol{C}^1_{3\times30\times N}$ is the preprocessed signal from transmitter antenna 1 and receiver antenna 1, 2, 3. The amplitude changes of the variance signal are due to the motion and other factors (e.g., environment noise), while the motion is the most strong one. Hence, we perform threshold processing for each element of variance matrix $\boldsymbol{V}_{3\times30\times L}$ as shown in Equation (4)

$$\boldsymbol{V}_{(i,j,k)} = \begin{cases} 1, & \boldsymbol{V}_{(i,j,k)} > \mu_1 \\ 0, & \text{otherwise}, \end{cases} \tag{4}$$

where μ_1 is the variance threshold and it is set according to the strength of motion to make the segmentation in the following steps robust. In our experiments, we set μ_1 to 0.1 experimentally. By the above threshold operation, the variance matrix is transformed into a 0-1 binary matrix. Then we reduct the binary matrix $\boldsymbol{V}_{3\times30\times L}$ into a 2D matrix $\boldsymbol{F}_{90\times L}$. Finally, the 2D matrix from the three spatial streams with a total of 90 subcarriers are superimposed to obtain the MSV $\boldsymbol{s}_{1\times L}$.

Since each value of the MSV is obtained by summing the binary values of all 90 subcarriers, the MSV can combine the information from all three spatial streams. Compared to selecting a few subcarriers, MSV is much more robust. The magnitude of MSV represents the degree of change in human motion. We predict the user keeping a stationary state and the corresponding signal change is within range in normal indoor environment when the MSV amplitude is close to 0. Fig. 3(b) shows the MSV derived from the raw signal using the algorithm above, in which the motion and static state is much more detectable than that in Fig. 3(a).

The original 3D complex matrix is transformed into a real vector, which can greatly condense the data size and promote calculation efficiency. In addition, through the data transformation, the trend of signal changes is further strengthened, which is more conducive for the accurate state segmentation in the following step.

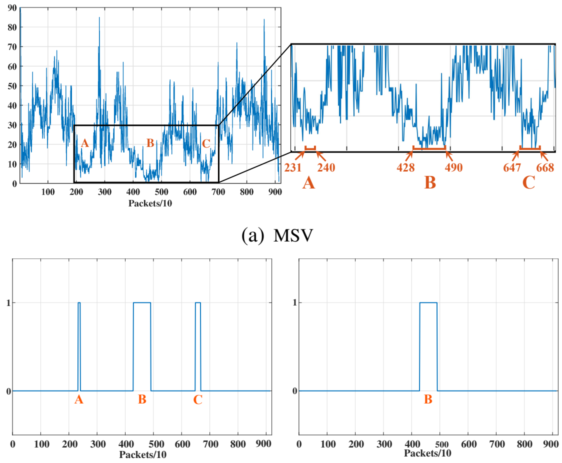

(a) MSV

(b) Pre-segmentation (c) Final segmentation

Fig. 4: State detection and segmentation

2) State Detection and Segmentation: Once the MSV is obtained, we need to perform state detection and segmentation to get the bio-electromagnetic information. Based on the observation from Fig. 3(b), we can see that there is obviously different signal pattern changes from the MSV. In this part, we propose a threshold-based adaptive signal segmentation algorithm to obtain the static state through MSV.

Though the difference between the motion and stationary states becomes more obvious in MSV, there are still some interferences, which can cause misjudgment of the start and end moment of the stationary state. Hence, a Gaussian-weighted moving average filter is used to smooth the MSV $\boldsymbol{s}$ to $\boldsymbol{s}'$. Then the smoothed vector $\boldsymbol{s}'$ is preliminarily segmented by a threshold-based adaptive signal segmentation algorithm as shown in Equation (5)

$$\boldsymbol{p}_{(m)} = \begin{cases} 1, & \boldsymbol{s}'_{(m)} < 2 \cdot min(\boldsymbol{s}') + \mu_2 \\ 0, & \text{otherwise}, \end{cases} \tag{5}$$

where $\boldsymbol{p}$ is the preliminary segmentation result, μ_2 is a predefined threshold for segmentation which we set to 1 empirically. Since the level of motion strength varies from user to user, the threshold in Equation (5) should be an adaptive value instead of a fixed one. The thresholding in Equation (5) is designed to adaptively divide the MSV into motion and stationary states based on the minimum value of the given MSV.

Actually, we perform the segmentation by decomposing the motion state into numerous static sub-states that last for a period of time, by which any static state can be detected. The duration of the sub-state will affect the accuracy of segmentation. Fig. 4(a) shows the MSV obtained from another raw data. As shown in Fig. 4(a), the three valley ranges denoted as A, B and C indicate that the user is stationary in these three periods. The preliminary segmentation result is shown in Fig. 4(b), which is decided by our previous filtering algorithm and MSV algorithm based on the sliding window. The theoretical minimum number of packets that can be detected as stationary state for physiological information extraction depends on the product of the window sizes of all previous sliding window operations. Specifically, the window size of the Hampel identifier during the data preprocessing is 5, the window size in Equation (3) is 10, and the window size of the Gaussian-weighted moving average filter before Equation (5) is 10. Hence, the theoretical minimum number of data packets in our experiments is 500. B contains enough (more than 500) packets to extract physiological information, while A and C are considered as anomalous noise due to the number of packets less than 500. We propose to use the Hampel identifier to remove these short time periods, which can extract sufficient physiological information to get the final segmentation result as shown in Fig. 4(c).

3) Bio-electromagnetic Information Combination: Once we get the segmentation of the static state, we can determine the start and end indexes of the data packets for the extraction of the valid bio-electromagnetic information. As stated in Section III-B, the CSI from nine spatial streams is used as a unique feature to identify individuals. Therefore, each person's bio-electromagnetic information can be represented by a 1×270 feature vector. Fig. 5 shows the CSI containing the bio-electromagnetic information in 3D (i.e., Amplitude-Packet Index-Subcarrier Index), these are 500 packets from three different individuals and each packet has 270 CSI subcarriers. As we can see, the attenuation of CSI sequences of different individuals on different subcarriers has unique characteristics, while the attenuation of the CSI sequences of the same individual on different subcarriers at different packets remains relatively stable.

D. Person Identification

Although the combined bio-electromagnetic information is successfully extracted from the static state, there is inevitably some subtle action noise produced by people. Principal Component Analysis (PCA) is leveraged to de-noise the data, which can preserve 99% of the primary information in the original data. Using PCA, we cannot only remove the action noise but also condense the data size while preserving the original information as much as possible. The computational efficiency can be improved in the following steps.

We feed the combined bio-electromagnetic data into the neural network for hidden feature extraction. The neural network consists of a sequence input layer, an LSTM layer, a full connection layer, a softmax layer, and a classification

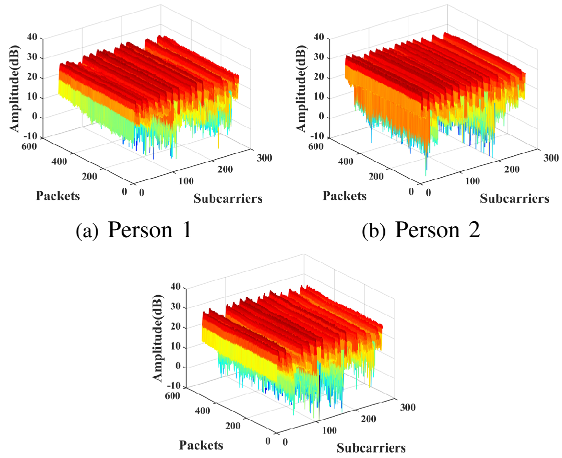

(a) Person 1 (b) Person 2

(c) Person 3

Fig. 5: The feature vectors of different people

output layer. We feed 10 consecutive packets as one training sample into the neural network for training. Although one packet can describe a single individual, we find that using 10 consecutive packets training is significantly better than using a single packet. Finally, the softmax layer is used for multi-classification tasks to achieve person identification.

IV. Experiments and Evaluation

A. Experiment Setup

(a) *Env 1*: Square (b) *Env 2*: Corridor (c) *Env 3*: Office

Fig. 6: Experimental environments

We used two laptops (ThinkPad T400) installed with Ubuntu 14.04 LTS as the transceivers, both of which are equipped with Intel 5300 NIC. Specifically, one laptop with three external omnidirectional antennas acts as the transmitter and another laptop with the same configuration acts as the receiver. Two laptops installed with CSI Tool [20] work in IEEE 802.11n Monitor mode on Channel 64 at 5.32 GHz. We conducted the experiments with a group of 14 people in three different environments. The details of environments and volunteers are shown in Fig. 6 and Table I, respectively. Each packet we received has a total of 270 subcarriers from nine spatial streams. The transmission rate is set to be 1,000 Hz. The volunteer is asked to stand still at the midpoint of the LoS to get the training sets and each volunteer collects 64,000 training samples. In the testing phase, the volunteer can walk along or vertical to the LoS, but the volunteer's walking path should contain the midpoint of the LoS for segmenting the valid bio-electromagnetic information. Each group of data contains about 3,000 samples. The dataset is collected with appropriate written informed consent and human subjects approval and is publicly available on Github (https://github.com/MDHan/WiID.git) for non-commercial scientific research.

TABLE I: The details of the volunteers

ID	Gender	Height (cm)	Weight (kg)	ID	Gender	Height (cm)	Weight (kg)
1	Female	166	49	8	Male	174	72.5
2	Male	170	68	9	Male	180	79
3	Female	166	52	10	Female	174	62
4	Male	180	75	11	Female	165	55
5	Male	173	63.5	12	Male	182	81
6	Female	157	56	13	Female	155	52
7	Male	178	92.5	14	Male	171	67

B. Impact of Different Configurations

The volunteer number, spatial stream number, transceiver distance, and transceiver height are 7, 9, 4m, and 0.7m, respectively. All results in Table II are the average values of three experiments. In addition, we have performed extensive experiments to evaluate the performance of the proposed method in *Env 2* (Corridor). The experimental parameters are consistent with the above except for the variables we validated.

TABLE II: The impact of different configuration parameter

Factor	Value	Accuracy	Factor	Value	Accuracy
Env	Env 1	85.02%	Spatial Stream	1	91.54%
	Env 2	97.12%		3	93.45%
	Env 3	95.82%		9	97.12%
Transceiver Height	0m	85.94%	Transceiver Distance	2m	91.62%
	0.7m	97.12%		4m	97.12%
	1.2m	80.45%		6m	92.64%

Environments: The effect of multipath can be fully reflected in this experiment. Since our identification system works based on the attenuation of WiFi signals, more person physiological information from CSI can be extracted in the environments with more multipaths. The square environment has little multipath due to the absence of other obstacles, while indoor environments such as corridors and offices are rich in multipath information. Less physiological information can be captured in *Env 1*. Therefore the accuracy in *Env 1* is much lower than that in *Env 2* and *Env 3*.

Spatial Stream Amount: The spatial streams number represents the number of antenna pairs used between the transmitter (Tx) and the receiver (Rx). 1 means one Tx antenna and one Rx antenna are used, 3 means one Tx antenna and three Rx antennas are used, and 9 means three Tx antennas and three Rx antennas are used. Since the spatial streams are independent of each other, the more spatial streams there are, the more physiological information can be extracted. Fine-grained CSI of spatial streams can capture more bio-electromagnetic information of the human body in terms of different sights to improve the robustness of person identification.

Distance between Transceivers: We place the transceiver at different horizontal distances to simulate the true indoor environment and evaluate the best configuration parameters about the transceiver for person identification. The sensing accuracy of WiFi signals gradually decreases with the increasing distance between the transceiver. Person identification achieves the best accuracy of 97.12% in $4m$ and the accuracy decrease to 92.64% in $6m$. Once the distance is up to $8m$, the accuracy of person identification quickly decreases and cannot satisfy the requirement of real application.

Height between Floor and Transceiver: The strong sensing zone covered by WiFi signals depends on the height of the transceiver. From the experimental results of different heights, the best accuracy of person identification is 97.12% in $0.7m$. In other words, in the strong sensing zone, the stronger signal changes can be reflected when WiFi signals penetrate through the human body.

Apparel Changing and Stuff Carrying: The clothes people wear are mainly made of non-conductor materials such as cotton and polyester. In such cases, the apparel has no effect on the propagation of electromagnetic waves. However when there are some conductor materials (e.g., metal zipper) on the clothes, these materials will have a slight effect on the extracted bio-electromagnetic information, and the effect can be removed by using classical signal processing methods, such as PCA. The effect on bio-electromagnetic information caused by the stuff in hand has a similar conclusion.

C. Impact of Group Size

The state-of-the-art WiFi person identification systems are mainly for the smart home, office and other scenarios where the crowd size is relatively small [12, 13, 18]. We conducted three experiments with $N(2 \leq N \leq 14)$ randomly selected volunteers to investigate the performance of our method on different group sizes in *Env 2*. The average accuracy of the experiments are shown in Fig. 7. When the volunteers number increases from 2 to 14, the identification accuracy decreases from 100% to 95.25%. As we all know, the similar physiological information of individuals will increase the difficulty of identification with increasing the number of volunteers. However, even in a group of 14 volunteers, the identification accuracy of our method is still above 95%, which indicates that our approach can achieve robust person identification in small crowd sizes.

D. Performance Comparison

The WiID is compared with the state-of-the-art bio-electromagnetic based WiFi person identification system WiPIN [19] in *Env 2*. Since WiPIN only works when the user is completely stationary, we evaluate it using the stationary data in our dataset. As shown in Fig. 8, though the mean accuracy of WiPIN and our approach (WiID/M) tends to decline with the group size increase, our proposed WiID has a significant performance improvement over WiPIN. Our approach is superior to WiPIN for two reasons. The first reason is that the motion noise can seriously affect the performance of

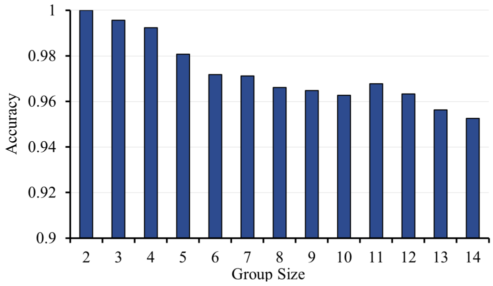

Fig. 7: Accuracy of different group size

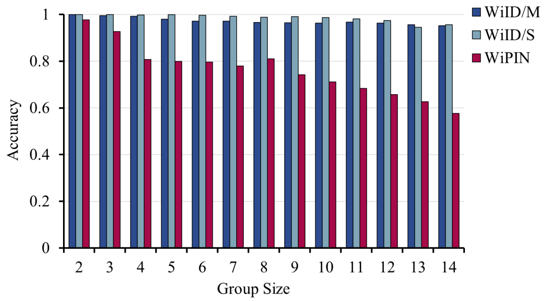

Fig. 8: Performance comparison

the WiPIN algorithm, while our proposed method are designed to remove motion noise and only preserve information in the stationary state. The second reason is that WiPIN only utilizes the data from 30 subcarriers of one spatial stream and uses the simple SVM algorithm for classification. When the group size increases, using single spatial stream data with the SVM algorithm fails to extract sufficient features to distinguish multiple people. However, our method utilizes all 270 subcarriers of nine spatial streams with the LSTM based algorithm and is able to extract richer features.

Our method also achieves better performance than WiPIN using only the stationary data (WiID/S) and remains stable, especially in the case of larger group size. Since the data collected in dynamic scenes may contain motion noise, which affects the accuracy of identification, our approach has better performance in the stationary scenes than in the dynamic scenes.

V. Conclusion

In this paper, the WiID, a novel WiFi-based moving person identification method, has been proposed to map WiFi CSI from different spatial streams with human physiological characteristics, by which accurate person identification can be successively achieved. Specially, short-time segmentation is carried out through an MSV design in our work, which facilitates our method to perform well with moving individual identification. Experimental results in different indoor and outdoor scenarios have shown that WiID can achieve accurate and robust person identification under various system deployments.

Acknowledgment

This work is supported by NSF of Shandong (No. ZR2021LZH010, No.ZR2020LZH015, No.ZR2020MF042) and Scientific Research Leader Studio of Jinan (No.2021GXRC081).

References

[1] Fusang Zhang, Kai Niu, Jie Xiong, Beihong Jin, Tao Gu, Yuhang Jiang, and Daqing Zhang, "Towards a diffraction-based sensing approach on human activity recognition," *Proceedings of the ACM on Interactive, Mobile, Wearable and Ubiquitous Technologies*, vol. 3, no. 1, pp. 1–25, 2019.

[2] Zhenghua Chen, Le Zhang, Chaoyang Jiang, Zhiguang Cao, and Wei Cui, "WiFi CSI based passive human activity recognition using attention based BLSTM," *IEEE Transactions on Mobile Computing*, vol. 18, no. 11, pp. 2714–2724, 2018.

[3] Dan Wu, Ruiyang Gao, Youwei Zeng, Jinyi Liu, Leye Wang, Tao Gu, and Daqing Zhang, "FingerDraw: Sub-wavelength level finger motion tracking with WiFi signals," *Proceedings of the ACM on Interactive, Mobile, Wearable and Ubiquitous Technologies*, vol. 4, no. 1, pp. 1–27, 2020.

[4] Yili Ren, Zi Wang, Sheng Tan, Yingying Chen, and Jie Yang, "Winect: 3D human pose tracking for free-form activity using commodity WiFi," *Proceedings of the ACM on Interactive, Mobile, Wearable and Ubiquitous Technologies*, vol. 5, no. 4, pp. 1–29, 2021.

[5] Heba Abdelnasser, Moustafa Youssef, and Khaled A Harras, "Wigest: A ubiquitous WiFi-based gesture recognition system," in *2015 IEEE Conference on Computer Communications (INFOCOM)*, 2015, pp. 1472–1480.

[6] Hao Wang, Daqing Zhang, Yasha Wang, Junyi Ma, Yuxiang Wang, and Shengjie Li, "RT-Fall: A real-time and contactless fall detection system with commodity WiFi devices," *IEEE Transactions on Mobile Computing*, vol. 16, no. 2, pp. 511–526, 2016.

[7] Yan Wang, Jian Liu, Yingying Chen, Marco Gruteser, Jie Yang, and Hongbo Liu, "E-eyes: Device-free location-oriented activity identification using fine-grained WiFi signatures," in *Proceedings of the 20th Annual International Conference on Mobile Computing and Networking*, 2014, pp. 617–628.

[8] Baoqi Huang, Runze Yang, Bing Jia, Wuyungerile Li, and Guoqiang Mao, "A theoretical analysis on sampling size in WiFi fingerprint-based localization," *IEEE Transactions on Vehicular Technology*, vol. 70, no. 4, pp. 3599–3608, 2021.

[9] Han Zou, Ming Jin, Hao Jiang, Lihua Xie, and Costas J Spanos, "WinIPS: WiFi-based non-intrusive indoor positioning system with online radio map construction and adaptation," *IEEE Transactions on Wireless Communications*, vol. 16, no. 12, pp. 8118–8130, 2017.

[10] Chen Chen, Yan Chen, Hung-Quoc Lai, Yi Han, and KJ Ray Liu, "High accuracy indoor localization: A WiFi-based approach," in *2016 IEEE International Conference on Acoustics, Speech and Signal Processing (ICASSP)*, 2016, pp. 6245–6249.

[11] Hang Li, Xi Chen, Ju Wang, Di Wu, and Xue Liu, "DAFI: WiFi-based device-free indoor localization via domain adaptation," *Proceedings of the ACM on Interactive, Mobile, Wearable and Ubiquitous Technologies*, vol. 5, no. 4, pp. 1–21, 2021.

[12] Yunze Zeng, Parth H Pathak, and Prasant Mohapatra, "WiWho: WiFi-based person identification in smart spaces," in *2016 15th ACM/IEEE International Conference on Information Processing in Sensor Networks (IPSN)*, 2016, pp. 1–12.

[13] Jin Zhang, Bo Wei, Wen Hu, and Salil S Kanhere, "WiFi-id: Human identification using WiFi signal," in *2016 International Conference on Distributed Computing in Sensor Systems (DCOSS)*, 2016, pp. 75–82.

[14] Jie Wang, Yunong Zhao, Xinxin Fan, Qinghua Gao, Xiaorui Ma, and Hongyu Wang, "Device-free identification using intrinsic CSI features," *IEEE Transactions on Vehicular Technology*, vol. 67, no. 9, pp. 8571–8581, 2018.

[15] Han Zou, Yuxun Zhou, Jianfei Yang, Weixi Gu, Lihua Xie, and Costas Spanos, "WiFi-based human identification via convex tensor shapelet learning," in *Proceedings of the AAAI Conference on Artificial Intelligence*, 2018, vol. 32.

[16] Belal Korany, Hong Cai, and Yasamin Mostofi, "Multiple people identification through walls using off-the-shelf WiFi," *IEEE Internet of Things Journal*, vol. 8, no. 8, pp. 6963–6974, 2020.

[17] Lei Zhang, Cong Wang, and Daqing Zhang, "Wi-PIGR: Path independent gait recognition with commodity WiFi," *IEEE Transactions on Mobile Computing*, 2021.

[18] Qinyi Xu, Yan Chen, BeiBei Wang, and KJ Ray Liu, "Radio biometrics: Human recognition through a wall," *IEEE Transactions on Information Forensics and Security*, vol. 12, no. 5, pp. 1141–1155, 2017.

[19] Fei Wang, Jinsong Han, Feng Lin, and Kui Ren, "WiPIN: Operation-free passive person identification using WiFi signals," in *2019 IEEE Global Communications Conference (GLOBECOM)*, 2019, pp. 1–6.

[20] Daniel Halperin, Wenjun Hu, Anmol Sheth, and David Wetherall, "Tool release: Gathering 802.11n traces with channel state information," *ACM SIGCOMM Computer Communication Review*, vol. 41, no. 1, pp. 53–53, 2011.

[21] Lei Zhang, Cong Wang, Maode Ma, and Daqing Zhang, "WiDIGR: Direction-independent gait recognition system using commercial WiFi devices," *IEEE Internet of Things Journal*, vol. 7, no. 2, pp. 1178–1191, 2019.

[22] David Tse and Pramod Viswanath, *Fundamentals of wireless communication*, Cambridge university press, 2005.

[23] Sami Gabriel, RW Lau, and Camelia Gabriel, "The dielectric properties of biological tissues: II. Measurements in the frequency range 10 Hz to 20 GHz," *Physics in Medicine & Biology*, vol. 41, no. 11, pp. 2251, 1996.

[24] Andreas Christ, Anja Klingenbock, Theodoros Samaras, Cristian Goiceanu, and Niels Kuster, "The dependence of electromagnetic far-field absorption on body tissue composition in the frequency range from 300 MHz to

6 GHz," *IEEE Transactions on Microwave Theory and Techniques*, vol. 54, no. 5, pp. 2188–2195, 2006.

[25] Ilka Dove, "Analysis of radio propagation inside the human body for in-body localization purposes," M.S. thesis, University of Twente, 2014.